

# THE ROLE OF THE BASE PERIOD IN EVALUATING TELECONNECTION INDICES AND STRENGTHS, AND HOW TO ELIMINATE IT IN THE SNAPSHOT FRAMEWORK USING LARGE ENSEMBLES

Tímea Haszpra<sup>1,2</sup>, Gábor Drótos<sup>2,3</sup>, Dániel Topál<sup>4</sup>, Mátyás Herein<sup>2</sup>

<sup>1</sup> Department of Theoretical Physics, Eötvös Loránd University, Budapest, Hungary, <sup>2</sup> MTA–ELTE Theoretical Physics Research Group, Eötvös Loránd University, Budapest, Hungary, <sup>3</sup> Instituto de Física Interdisciplinar y Sistemas Complejos (CSIC–UIB), Palma de Mallorca, Spain, <sup>4</sup> Institute for Geological and Geochemical Research, Research Center for Astronomy and Earth Sciences, Budapest, Hungary

## 1. Introduction

Different teleconnection index time series are obtained even within a single member of a large ensemble simulation if different base periods are chosen. This also has an effect on the apparent strength of teleconnections. In this study, the reasons behind this caveat are discussed and exemplified for the Arctic Oscillation. Additionally, a solution is presented in the so-called snapshot framework using large ensemble simulations.

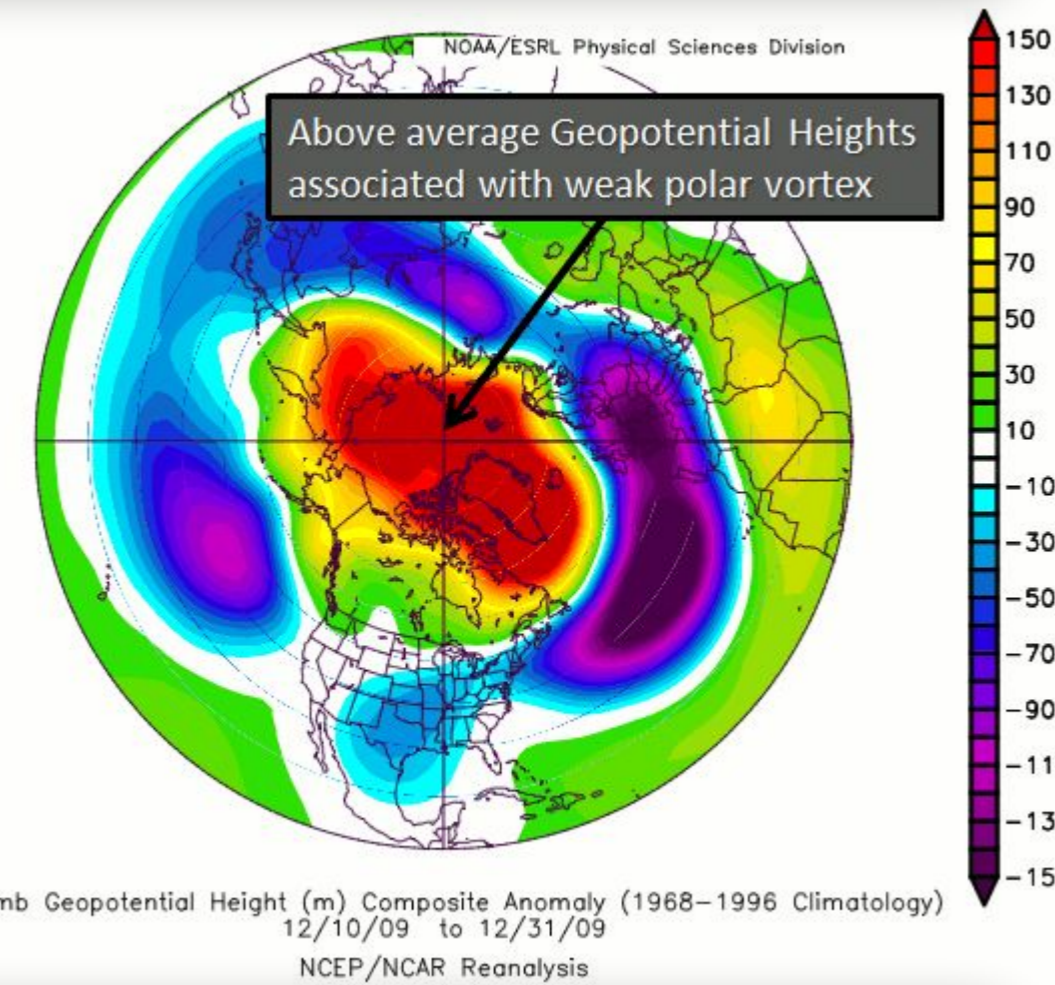
## 2. Arctic Oscillation (AO)

- „ring-like” anomaly in the sea-level pressure (SLP)/geopotential fields over 20–90° N with +(-) sign in the Arctic and opposite sign at 37–45° N
- AO index (AOI): characterizes circulation pattern, quantifies the rate at which the Arctic air gets to the mid-latitudes

### 2.1. The AO's teleconnections

In (-) phase [(+) phase: opposite]

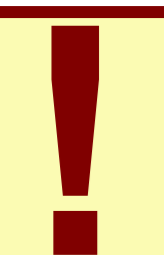
- weaker polar vortex
- weaker upper level winds/westerlies
- U.S., N. Europe, Asia: Arctic air reaches more southerly latitudes → cold winter
- Mediterranean: storms



<https://climate.ncsu.edu/climate/patterns/nao>

### 2.2. Traditional definition and computation

- AO's loading pattern: the leading mode of the empirical orthogonal function (EOF) analysis of sea-level pressure (SLP) from 20° to 90° N for a given base period
- AO index (AOI) time series: SLP anomalies projected on this loading pattern (principal components, PCs), standardized for the base period
- AO amplitude: std. dev. of the PCs for the base period
- strength of AO teleconnections: correlation coefficient between two time series:  $r(\text{AOI, other meteorological variable})$



Quantities are computed over the time dimension and for a given base period → subjective!

## 3. The role of the base period

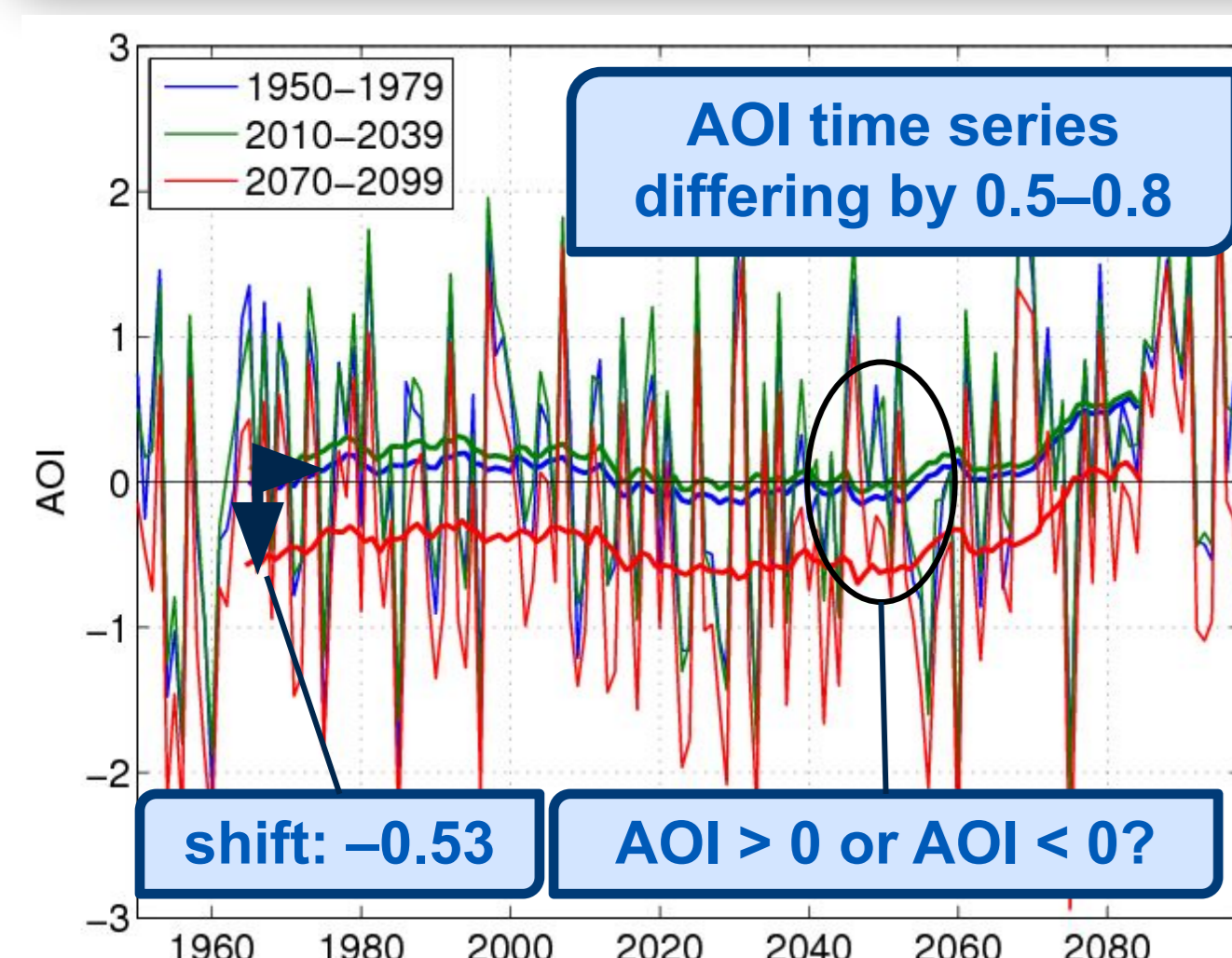


Fig. 1. AOI time series for the 1st member of the MPI-GE for RCP8.5 calculated by using different base periods (legend). The time series of the 30-year moving mean (thick solid lines) are also plotted.

Can any of the AOI time series be considered to be „the real one”? NO



## 3.1. Explanation (for any EOF-based phenomena)

1. The EOF1 loading pattern represents a standing oscillation pattern, treated as constant within the studied time interval
  - The index (e.g. AOI) shows how this pattern oscillates in time.
  - When the climate changes, stationarity cannot be assumed: neither the structure of the oscillation pattern nor the amplitude of the oscillation remain constant.

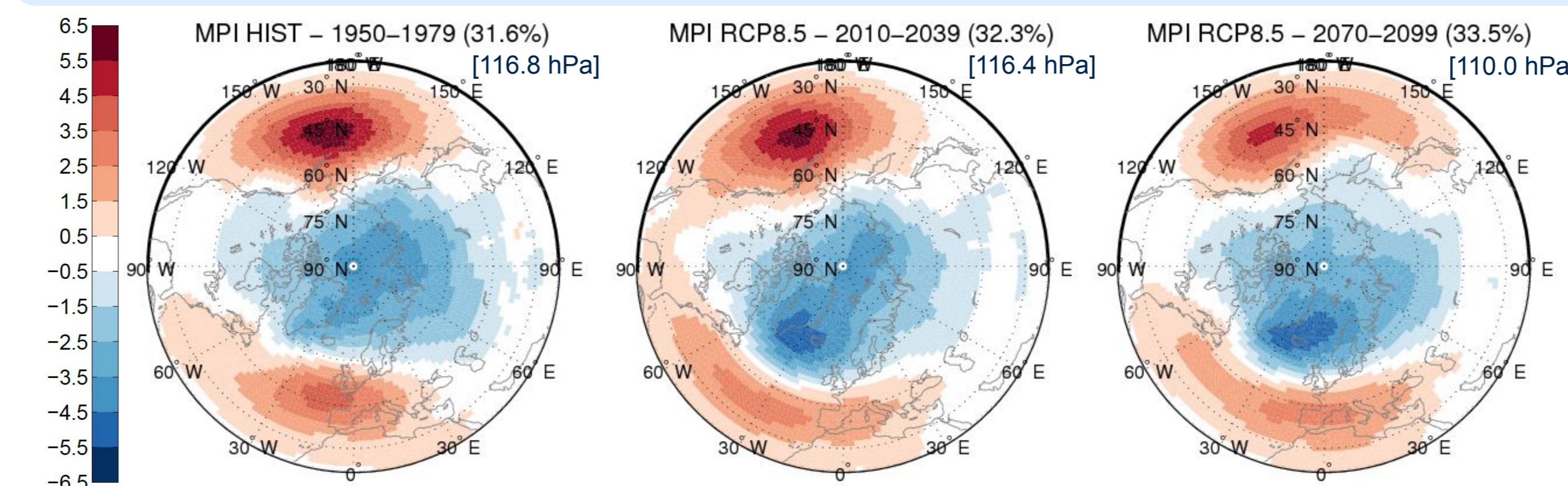


Fig. 2. Changes in the oscillation pattern and amplitude using different base periods. DJF mean SLP anomalies [hPa] regressed onto the 1st EOF mode with explained variance indicated in parenthesis and amplitude indicated in brackets for the 1st member of the MPI-GE for the RCP8.5 scenario.

2. Any shift in the index time series originates from a change in the mean state of the climate system (e.g., temporal mean of the SLP field), which is the center of the oscillation (AOI = 0) described by the given EOF mode.

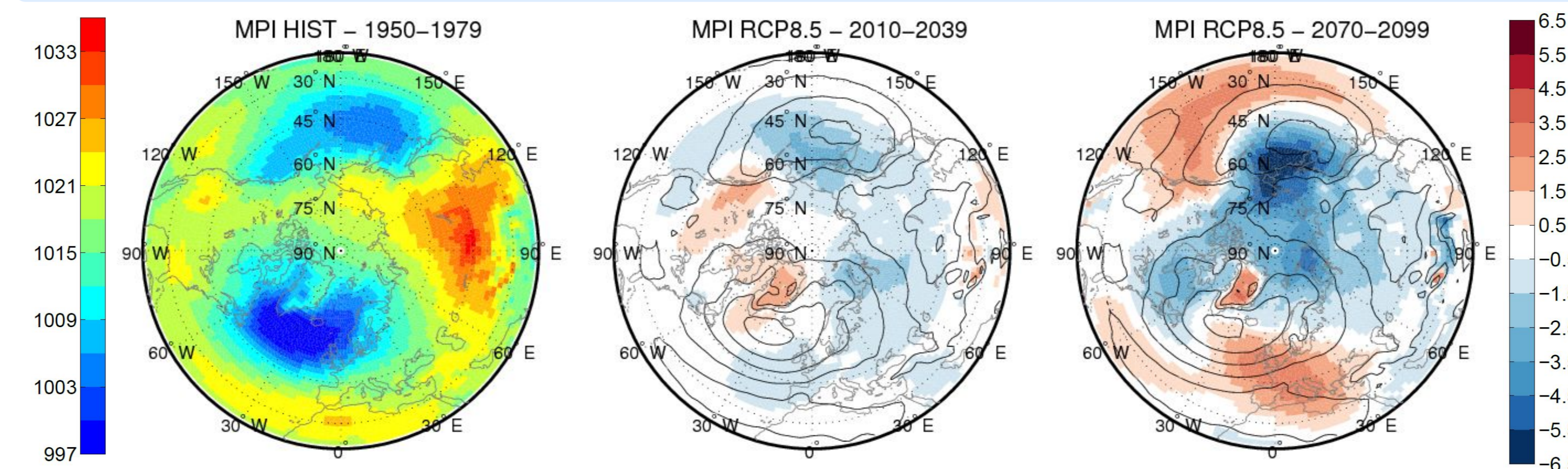


Fig. 3. Changes in the mean SLP field. DJF mean SLP fields [hPa] (left with jet contour, and middle and right with black contour lines) and the difference of the DJF mean SLP fields from that of 1950–1979 [hPa] (middle and right with red-blue contours).

## 3.2. Quantification of the difference (Haszpra et al. 2020)

- Shift of the AOI time series using base periods  $b_1$  and  $b_2$ : the mean value of the AOI time series derived via  $b_2$  for  $b_1$ :

$$\sigma_{b_2}^{-1} |\Delta\text{SLP}| \cos\theta$$

- $\sigma_{b_2}$ : std. dev. of the PC time series for  $b_2$
- $\Delta\text{SLP}$ : diff. field between the mean SLP field of  $b_1$  and  $b_2$ ,
- $\theta$  denotes the angle between the  $\Delta\text{SLP}$  field and the EOF1 loading pattern for  $b_2$  (both considered to be vectors)

- For Fig. 1 with  $b_1 = 1950–1979$  and  $b_2 = 2070–2099$ :  $\sigma_{b_2} = 110.0$  hPa,  $|\Delta\text{SLP}| = 117.0$  hPa and  $\theta = 120^\circ \rightarrow \text{shift} = -0.53$  (in harmony with the value of the 30-year mean red curve for 1965)

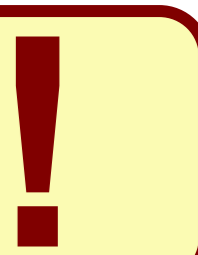
## Utilized data and abbreviations

- MPI-GE: Max Planck Institute Earth System Model 100-member Grand Ensemble
- CESM: Community Earth System Model 40-member Large Ensemble
- HIST: historical experimental design scenario, 1950–2005
- RCP2.6, 4.5, 8.5: Representative Concentration Pathway scenarios, 2006–2100

## 4. The snapshot framework – the solution

- Large ensembles: correctly characterize the set of states permitted by the climate system at each time instant after convergence time, e.g.:
- ensemble mean = instantaneous mean state of the system
- ensemble std. dev., EOF = quantifying possible instant. internal variability

Compute every statistics across the ensemble at each time instant! → time-dependence can be monitored



### 4.1. Snapshot EOF (SEOF, Haszpra et al. 2020)

- EOF analysis along the ensemble dimension at each time instant.
- The SEOF1 mode characterizes a kind of internal variability of the climate around its mean state at the given time instant.
- The results at any time instant are only affected by the number of ensemble members utilized.
- Results in:

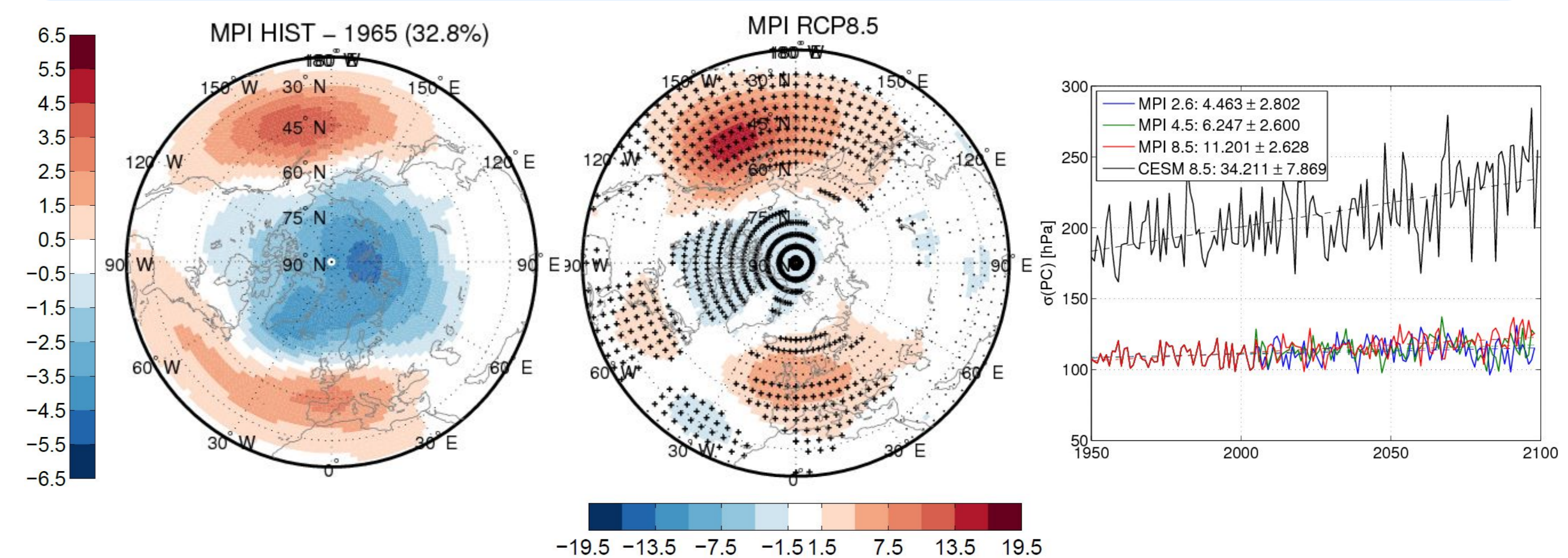


Fig. 4. Instantaneous oscillation patterns (DJF mean SLP anomalies [hPa] regressed onto the 1st SEOF mode with explained variance indicated in parenthesis, left), their time-dependence (linear trend [ $10^{-3}$  hPa yr $^{-1}$ ] in the regressed DJF mean SLP anomalies 1950–2100, middle), and time-dependence of the oscillation amplitude (std. dev. of the PCs, right).

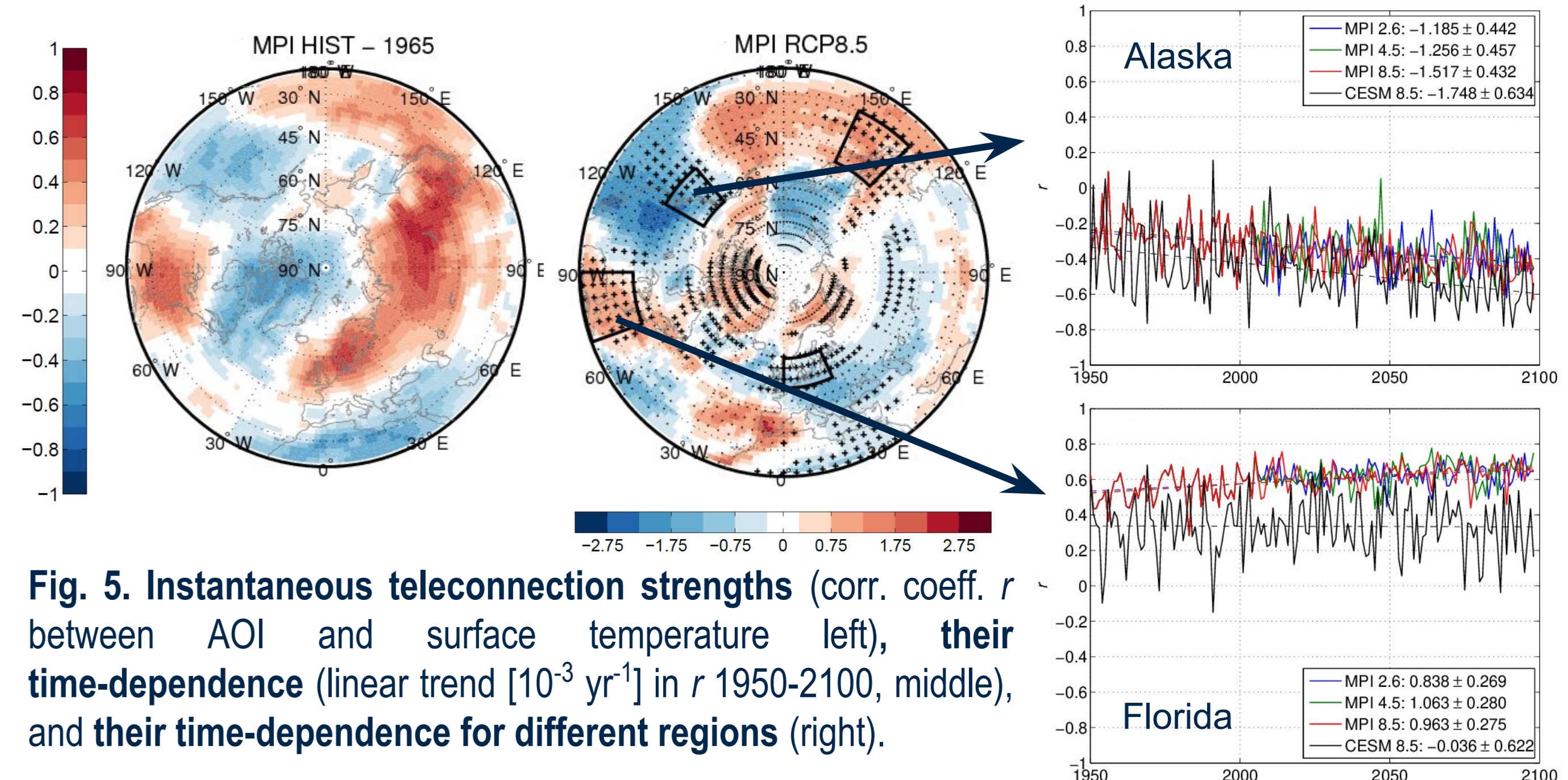


Fig. 5. Instantaneous teleconnection strengths (corr. coeff.  $r$  between AOI and surface temperature left), their time-dependence (linear trend [ $10^{-3}$  yr $^{-1}$ ] in  $r$  1950–2100, middle), and their time-dependence for different regions (right).

### Reference

Haszpra, T., Topál, D., Herein, M. (2020): On the time evolution of the Arctic Oscillation and related wintertime phenomena under different forcing scenarios in an ensemble approach. *J. Climate*, doi:10.1175/JCLI-D-19-0004.1

### Acknowledgments

This work was supported by the János Bolyai Research Scholarship of the Hungarian Academy of Sciences, by the National Research, Development and Innovation Office – NKFIH under grants PD-121305, PD-132709, FK-124256, K-125171 and by the ÚNKP-18-4 and ÚNKP-19-1 New National Excellence Program of the Ministry for Innovation and Technology.